Design and Optimization of a Single-Mode Multi-Core Photonic Crystal Fiber With the Nanorod Assisted Structure to Suppress the Crosstalk

Han Zhang, Guorui Wang, Jiwei Zhang, Fang Wang, Xin Yan, Xuenan Zhang, and Tonglei Cheng

***Abstract*—We propose and design a novel homogeneous nanorod-assisted multi-core photonic crystal fiber (NA-PCF), and it utilizes the flexibility of photonic crystal fiber (PCF) for air-hole design, NA-PCF applied to multi-core fiber (MCF) communication system. High refractive index nanorods are introduced in the center of the seven cores which are further surrounded by a periodical arrangement of air-holes. The air-holes and the nanorods work together to greatly suppress the crosstalk (XT) between the cores. By comprehensively balancing the influence of various parameters on XT, single-mode cutoff wavelength (λ_{cc}) and the effective mode field area (A_{eff}), simulation results show that the NA-PCF has a A_{eff} of about 70.26 μm^2, XT of about −50.58 dB/km, relative core multiplicity factor (RCMF) of 4.7 and λ_{cc} of 1530 nm. This designed structure targets applications in large-capacity long-distance MCF communication.**

***Index Terms*—Photonic crystal fiber, multi-core fiber, space division multiplexing, crosstalk.**

I. Introduction

With the exponentially growing demand on communication capacity of signal transmission systems, to further increase the capacity of transmission media has become an urgent need [1]. In recent years, through the use of time, wavelength and polarization-division multiplexing technologies, the transmission capacity of optical fibers has been significantly improved [2]. However, single mode single core fiber (SSF), as the most commonly used transmission media, is rapidly approaching its capacity limit due to the nonlinear Shannon effect [3]–[4]. To address this challenge, space division multiplexing (SDM) technology based on MCF has become a new focus [5]–[7], which is expected to overcome the physical limit of fibers, and solve the imminent transmission capacity crisis.

Making full use of the spatial dimension, MCF introduces a number of cores within a certain cladding diameter. To guarantee the large-capacity and long-distance transmission, MCF is required to increase the core number as large as possible, while keeping crosstalk (XT) as low as possible. XT, defined as the influence of a signal transmitting within a core on the signal transmitting in an adjacent core, can be characterized by the signal power ratio. To suppress XT, the most direct way is to increase the core distance, but within a limited fiber diameter, increasing the core distance will naturally reduce the core density. Therefore, XT suppression and a high density of cores are mutually restricted [6]. In this regard, a variety of solutions have been proposed to suppress XT in MCF, including the introduction of air-holes around the core, and the introduction of a low-refractive-index trench formed by low-doping materials around the core [8]–[11]. For these assisted structures, the basic design purpose is to form low refractive index regions between adjacent cores, enhancing the mode limitation to reduce the mode field overlap. However, the enhancing of the mode limitation often leads to a great increase in single mode cutoff wavelength (λ_{cc}), which must be taken into consideration during the MCF design in order to keep stable signal transmission in the communication band.

In this paper, we demonstrate a novel nanorod-assisted multi-core photonic crystal fiber (NA-PCF) for large-capacity and long-distance transmission. Drawing on the design flexibility of photonic crystal fiber (PCF) [12], air-holes are arranged periodically around seven cores of a regular hexagon distribution, which effectively suppresses XT and limits the mode field between cores. In addition, high refractive index nanorods are introduced in the seven cores to further limit the mode field leakage without increasing λ_{cc}. By comprehensively balancing the influence of various parameters on XT, λ_{cc} and the average effective area A_{eff}, a set of suitable fiber parameters is chosen in this work and the corresponding NA-PCF features are investigated, confirming that the core density is greatly increased while satisfactorily suppressing XT and supporting single-mode transmission. The proposed NA-PCF has great application prospects for long-distance large-capacity communications.

Manuscript received May 25, 2021; revised June 8, 2021; accepted June 11, 2021. Date of publication June 15, 2021; date of current version July 12, 2021. This work was supported in part by the National Key Research and Development Program of China under Grant 2019YFB2204001, in part by the National Natural Science Foundation of China under Grant 61775032, in part by the Natural Science Foundation of Science and Technology Department of Liaoning Province under Grant 2020BS046, and in part by Fundamental Research Funds for the Central Universities under Grants N2104022, N180704006, N2004021, and N180408018, and 111 Project (B16009). *(Corresponding author: Tonglei Cheng.)*

Han Zhang, Guorui Wang, Jiwei Zhang, Fang Wang, Xin Yan, and Xuenan Zhang are with the State Key Laboratory of Synthetical Automation for Process Industries, College of Information Science and Engineering, Northeastern University, Shenyang 110819, China (e-mail: 1900747@stu.neu.edu.cn; wangguorui8188@hotmail.com; zhangjiwei_1997@163.com; wangfang@ise.neu.edu.cn; yanxin@ise.neu.edu.cn; zhangxuenan@ise.neu.edu.cn).

Tonglei Cheng is with the State Key Laboratory of Synthetical Automation for Process Industries, College of Information Science and Engineering, Northeastern University, Shenyang 110819, China and also with the Hebei Key Laboratory of Micro-Nano Precision Optical Sensing and Measurement Technology, Qinhuangdao 066004, China (e-mail: chengtonglei@gmail.com).

Digital Object Identifier 10.1109/JPHOT.2021.3089490

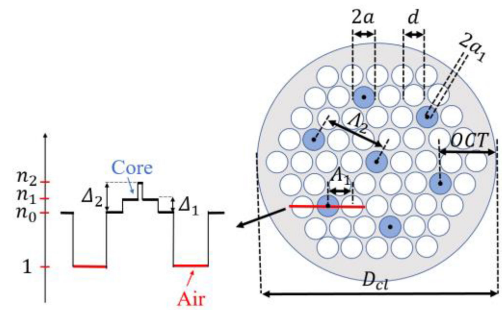

Fig. 1 Cross-section of the designed 7-core NA-PCF and refractive index profile of each core.

II. The Profile and Principle of NA-PCF

A. Profile of NA-PCF

Fig. 1 shows the cross-section and refractive index profile of the NA-PCF proposed in this paper. Seven cores are arranged in a regular hexagon, surrounded by a periodical arrangement of air-holes. The cladding is made of silica, and the refractive index n_0 is 1.444. Both the fiber core and the nanorods are made of GeO_2-doped silica [13], and by changing the doping concentration, the material refractive index is adjusted, which are respectively indicated by n_1 and n_2. The distance between the core and the air-hole, as well as the distance between adjacent air-holes are both indicated by Λ_1; the distance between cores is Λ_2 ($\Lambda_2 = \sqrt{7}\,\Lambda_1$); a, a_1 and d correspond to the core radius, the nanorod radius and the air-holes diameter; Δ_1 and Δ_2 respectively indicate the relative refractive index difference between core and cladding, and that between nanorod and cladding; the fiber diameter is D_{cl}, and outer cladding thickness (OCT) refers to the distance from the center of outer core to the edge of cladding [14].

B. XT of NA-PCF

For the proposed NA-PCF, the mode field distribution of each core is relatively independent, and only fundamental mode is supported by the relative refractive index difference between the core and the cladding. Assuming the power coupling coefficients of the middle core and the outer 6 cores are the same, expressed as $h^{(7)}$, and the initial power of the middle core is $P_1(0)$, according to weakly coupled fiber perturbation theory and power coupling theory [15]–[16], when the optical signal is excited from the middle core, the normalized power of the middle core and the outer cores can be expressed as [17]:

$$\frac{P_1(z)}{P_1(0)} = \frac{1+\exp\left(-7h^{(7)}z\right)}{7} \tag{1}$$

$$\frac{P_k(z)}{P_1(0)} = \frac{1-\exp\left(-7h^{(7)}z\right)}{7} \tag{2}$$

$P_k(z)$ (k = 2, 3, …,7) represents the power of the kth core, z represents the propagation length, and XT generated by the excitation of the middle core to the outer cores is:

$$XT_P{}^{(7)}(z) = \frac{1-\exp\left(-7h^{(7)}z\right)}{1+6\exp\left(-7h^{(7)}z\right)} \tag{3}$$

TABLE I
Initial Setting of Fiber Structure Parameters

Parameter	a	a_1/a	Λ_1	Λ_2	d	Δ_1	Δ_2
Value	4μm	0.1	15μm	39.7μm	8μm	0.28%	2.5%

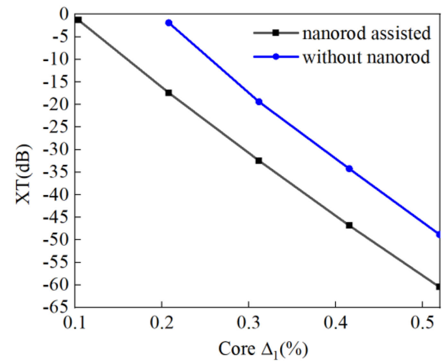

Fig. 2. XT dependence on Δ_1 of the NA-PCF and MCF without nanorod assistance.

The power coupling coefficient $h^{(7)}$ is:

$$h^{(7)} = \frac{1}{\sqrt{7}} \frac{2C_{12}^2}{\pi\sqrt{\left(\frac{\beta_2-\beta_1}{2}\right)^2 + C_{12}^2}} \tag{4}$$

Where β_1 and β_2 are the fundamental mode propagation constants of two adjacent cores, and C_{12} is the mutual coupling coefficient. For the middle core, the six outer cores all have a coupling effect on it, thus its XT is the largest. Therefore, this paper only calculates the XT of the middle core, and the goal is to control the value below −50 dB/km.

For the applications to long-distance high-capacity networks, three factors need to be taken into consideration: supporting single-mode transmission in the communication wavelength, having a larger A_{eff}, and suppressing XT. Because these three factors restrict with each other, it is necessary to carefully design the fiber parameters to achieve a balance [8]. This work aims to control XT of the center core less than −50 dB/km, A_{eff} bigger than 70 μm^2, and λ_{cc} of each core less than 1550 nm. A set of initial parameters are chosen through sufficient simulation calculations, as shown in Table I. The theoretical optimization is carried out at the wavelength of $\lambda = 1550$ nm, and the fiber length is set to be 1km.

C. Principle of Nanorod Assisted Structure

The introduction of the central high refractive index nanorod is to further increase the limiting effect of the fiber core on the mode field, the mode field is better restricted in the core and the interference between adjacent cores is reduced. A comparison of the XT suppression effect with and without the nanorod assistance is carried out when Δ_1 varies within a range of 0.1%–0.5%, as indicated by the black and blue lines in Fig. 2. It is clear that in the case of the same Δ_1, the black line is significantly lower than the blue one. Therefore, the introduction of nanorod

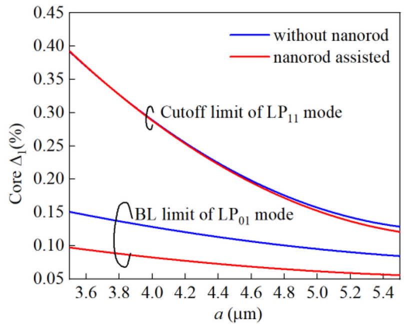

Fig. 3. Cutoff limit of LP_{11} mode at 1530 nm, $R_b = 140$ mm and BL limit of LP_{01} mode at $\lambda = 1625$ nm, $R_b = 30$ mm as function of a and Δ_1.

into the NA-PCF design produces a better effect on suppressing XT.

The influence of the central nanorods on λ_{cc} is taken into consideration during the fiber design. For a standard step-index fiber with core radius a, core refractive index n_{co} and cladding refractive index n_{cl}, λ_{cc} is defined as [18]–[19]:

$$\lambda_{cc} = 2\pi a(n_{co}^2 - n_{cl}^2)^{1/2}/V \tag{5}$$

It can be seen that a, n_{co}, n_{cl} are the direct factors that affect λ_{cc}. V stands for normalized frequency. In this paper, n_{co} and n_{cl} respectively correspond to the equivalent refractive index of the core and cladding, and λ_{cc} must be less than 1550 nm to guarantee single-mode transmission at the communication wavelength. However, it is difficult to accurately express the values of n_{co} and n_{cl} in numerical form, thus the cutoff conditions of LP_{01} and LP_{11} in the bending condition are used. The bending loss (BL) limit can be calculated by [20]:

$$BL = \frac{20}{\ln(10)}\frac{2\pi}{\lambda}imag(n_{eff}) \tag{6}$$

where imag(n_{eff}) means the imaginary parts of the n_{eff}. For single-mode transmission, when BL of LP_{01} is smaller than 0.5 dB/100 turns at bending radius (R_b) = 30 mm, $\lambda = 1625$ nm according to ITU-T recommendations G.655, which can be taken as LP_{01} mode being totally confined inside the core. Meanwhile, LP_{11} mode is regarded to be cutoff when BL of LP_{11} mode is larger than 1 dB/m at $R_b = 140$ mm, $\lambda = 1530$ nm according to the deployment configuration in IEC 60793-1-44 document. For the fiber with nanorod assistance and without nanorod structure, the cutoff limit of LP_{11} at 1530 nm ($R_b = 140$ mm) and BL limit of LP_{01} at 1625 nm ($R_b = 30$ mm) are respectively indicated in Fig. 3 by the blue and red lines. We can see that the LP_{11} mode curve does not change significantly, which proves that the introduction of the nanorods does not increase λ_{cc} of the NA-PCF. Meanwhile, the part enclosed by the same color line is called single mode operation region (SMOR) [21]–[22], and the core parameters chosen from this region can support single-mode transmission. With the introduction of the nanorods, the limiting effect on the mode field was enhanced, the BL limit of LP_{01} mode moved down, leading to an increased SMOR area and an enlarged parameter selection region.

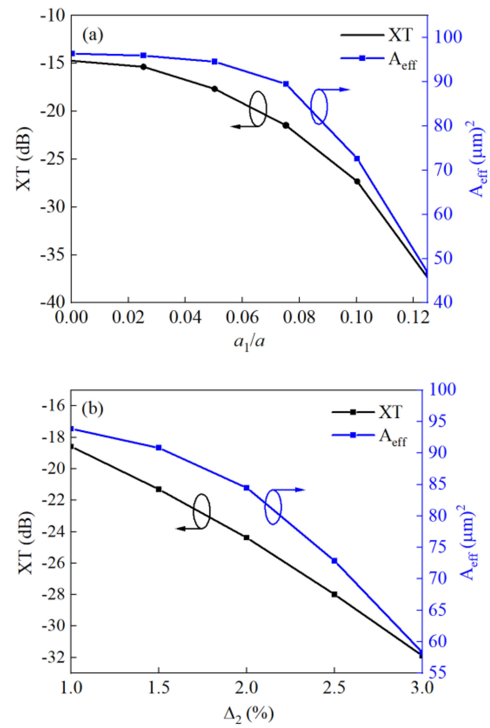

Fig. 4 (a) XT/A_{eff} dependence on a_1/a; (b) XT/A_{eff} dependence on Δ_2.

III. Selection of NA-PCF Parameters

A. Choice on a_1/a and Δ_2

The a_1/a and Δ_2 of the nanorods should be chosen appropriately to achieve the best effect on XT suppression. Fig. 4(a) and (b) respectively indicate the influence of a_1/a and Δ_2 on XT and A_{eff} of the central core. We can see that with the increase of these two values, XT and A_{eff} both decreases. Therefore, to suppress XT while enlarging A_{eff} should be well balanced during the parameter selection. To achieve the A_{eff} target of $\geq 70\ \mu m^2$, a/a_1 is to be selected as large as possible. Therefore, if the target A_{eff} is 70 μm^2, we have selected the following parameter: $a_1/a = 0.1$, $\Delta_2 = 2.5\%$. As have stated in the former discussion, the NA-PCF of as-set parameters can produce a better effect on suppressing XT without increasing λ_{cc}.

B. Choice on Λ_1 and d

The influence of the air-hole diameter d and air-hole pitch Λ_1 on XT and A_{eff} is investigated for the NA-PCF design. Fig. 5(a) shows the variation of XT with Λ_1 when d = 78 and 9 μm. We can see that the XT suppression effect gradually worsens with the increase of Λ_1, but strengthens with the increase of d. This is because when Λ_1 is small, the air-holes are closer to the core, which enhances the restraint effect on the surrounding mode field, and the larger d, the stronger the restriction effect. With the increase of Λ_1, the air-holes sparsely arranged around the core, weakening the restraint effect. Fig. 5(b) shows the variation of A_{eff} with Λ_1 when d = 78 and 9 μm. We can see that with the increase of Λ_1, A_{eff} firstly increases to the maximum, and then gradually decreases. The reason accounting for this phenomenon is that when d is fixed, with the increase of Λ_1

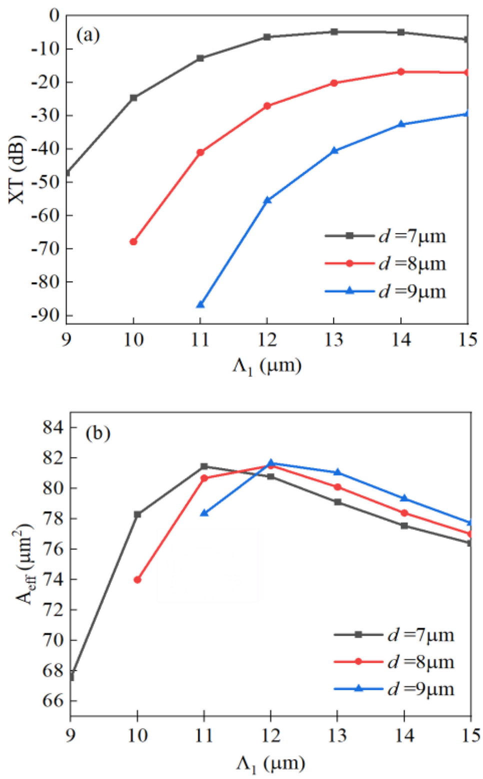

Fig. 5. (a) XT dependence on Λ_1 when d = 7 μm, 8 μm, 9 μm; (b)A_{eff} dependence on Λ_1 when d = 7 μm, 8 μm, 9 μm.

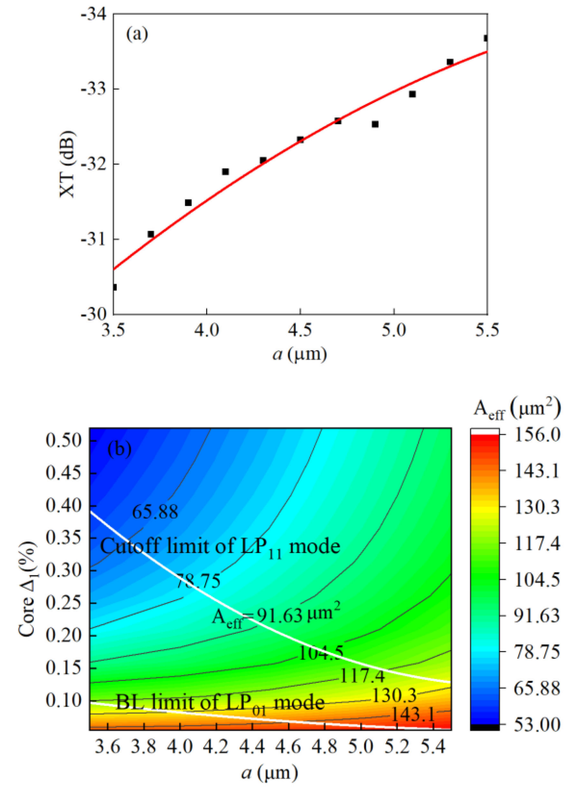

Fig. 6. (a) XT dependence on a; (b) A_{eff} of LP_{01} mode as a function of a and Δ_1.

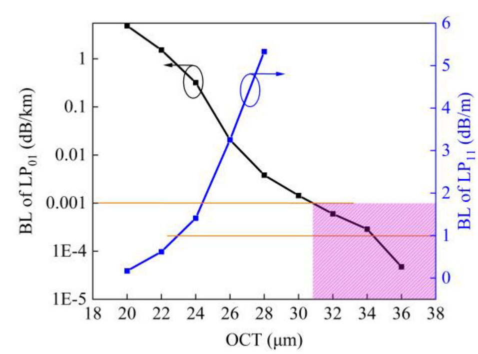

Fig. 7. Dependence of the outer core BL on OCT.

the air occupancy in the fiber is reduced, which weakens the mode field confinement ability and contributes to the increase of A_{eff}. After exceeding the maximum value, the arrangement of air-holes around the cores are relatively sparse, the mode field in the core diverges, thus A_{eff} decreases, leading finally to a relatively flattened curve trend. Therefore, during the NA-PCF design, Λ_1 should be minimized and d increased to suppress XT, relieving the mutual restriction between low XT and high core density. Meanwhile, the choice of Λ_1 and d should make A_{eff} approach the peak value as much as possible to obtain a larger A_{eff}. Moreover, considering the actual fabrication, the distance between the edge of adjacent air-holes should not be lower than 2 μm [23], for instance, when d is 9 μm, Λ_1 is at least 11 μm.

C. Choice on a and Δ_1

The influence of the core radius a and Δ_1 on XT suppression effect and A_{eff} is investigated. Fig. 6(a) shows the variation of XT with *a*, which changes by only 4 dB as a increases from 3.5 μm to 5.5 μm. As a result, a has a limited effect on XT, so the main concern is its influence on A_{eff}. Fig. 6(b) illustrates the A_{eff} of LP_{01} mode as a function of a and Δ_1, where the region enclosed by the upper and lower white lines is the SMOR area and where the black lines represent the contour lines of A_{eff} in the NA-PCF cores. We can see that A_{eff} grows as a increases and Δ_1 decreases. However, the value of Δ_1 directly influences the XT suppression effect, and the larger Δ_1, we can get lower XT, as presented in Fig. 2. Therefore, in order to meet the design targets, a larger Δ_1 should be selected in the SMOR area while the A_{eff} contour line is bigger than 70 μm^2.

D. Choice on OCT

For communication MCF, BL of the outer core is an important indicator, which is closely affected by OCT [14]. Moreover, because the refractive index of the coating material is larger than that of the cladding, if OCT is too thin, the coating with high refractive index will induce an additional loss of the outer cores. Therefore, the OCT value is vital in NA-PCF design process, which should ensure BL of LP_{01} at λ = 1625 nm and Rb = 140 mm smaller than 0.001 dB/km [14]. Fig. 7 demonstrates the BL of LP_{01} and LP_{11} mode, respectively indicated by the black and blue line. As mentioned before, to support single-mode transmission, BL of LP_{11} should be more than 1 dB/m as shown by the yellow lines in Fig. 7. It can be seen that when OCT is thinner than 31 μm, the BL requirement

TABLE II
SUITABLE NA-PCF PARAMETERS

Parameter	a	a_1/a	Λ_1	Λ_2	d	Δ_1	Δ_2	OCT
Value	3.94μm	0.1	15.4μm	40.7μm	7.1μm	0.39%	2.5%	31μm

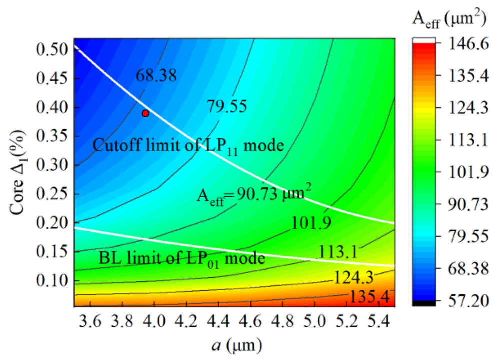

Fig. 8. A_{eff} of LP_{01} mode as a function of a and Δ_1.

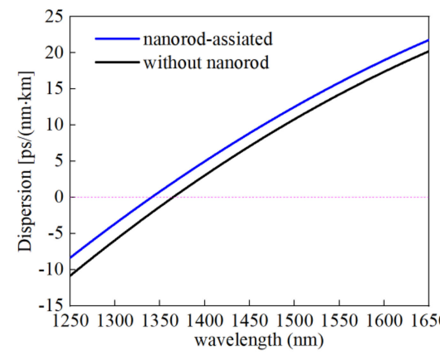

Fig. 9. The dispersion curve of LP_{01} mode as a function of wavelength.

can no longer be satisfied. Therefore, to meet the design target, OCT should be set as ≥ 31 μm to achieve the stable single-mode transmission.

IV. DETERMINATION OF FIBER PARAMETERS AND FIBER PERFORMANCE

A. Suitable NA-PCF Parameters

Through the above analysis, parameters should be carefully chosen to balance the three factors (XT, A_{eff} and λ_{cc}) for long-distance high-capacity communication. Parameters can be balanced according to requirements to achieve the performance indicators. In this paper, a set of appropriate parameters that meet the requirements are listed for reference. Firstly, the parameters of the nanorod and the air-holes around core were determined, after sufficient simulations, a_1 is selected to be 400 nm, $\Delta_2$2.5%, $\Lambda_1$15.4 μm, d 7.1 μm and OCT 31 μm. Based on it, the A_{eff} contour map is obtained, as shown by Fig. 8. Here Δ_1 is selected as 0.39% and a 3.94 μm, as indicated by the red dot. The fiber parameters selected in this paper for analysis are listed in Table 2.

B. Analysis on RCMF

The core density in MCF is characterized by the core multiplexing factor (CMF), which can be expressed as follows [14]:

$$CMF = \frac{N_{core}A_{eff}}{\pi(D_{cl}/2)^2} \tag{7}$$

where N_{core} is the number of cores in the fiber. For the purpose of comparison with SSF, the relative core multiplexing factor (RCMF) is introduced, which refers to the ratio of the CMF of MCF to the standard SSF (A_{eff} = 80 μm^2@1550 nm; the cladding diameter 125 μm). The RCMF expression is [14]:

$$RCMF = \frac{N_{core}A_{eff}}{\pi(D_{cl}/2)^2} / \frac{80}{\pi(125/2)^2} \tag{8}$$

TABLE III
THE OPTICAL PROPERTIES OF NA-PCF AT L = 1KM, λ = 1550 NM

Parameter	Unit	Fiber properties
XT	dB	-50.58
A_{eff}	μm^2	70.26
λ_{cc}	nm	1530
RCMF	-	4.7
Dispersion	ps/(nm*km)	14.06

The larger the value of RCMF, the better the space utilization rate of the optical fiber. Under the parameters of Table II, the RCMF of the designed NA-PCF is calculated to be 4.7, which indicates a greatly increased core density compared with the optical fibers reported previously [6],[24]. It proves that the proposed NA-PCF has bright application prospects for large-capacity communications.

C. Analysis on Chromatic Dispersion

Chromatic dispersion is a major factor causing optical pulse broadening in the transmission fibers. It is necessary to evaluate the effect of NA-PCF on fiber dispersion. Dispersion is made up of material dispersion and waveguide dispersion [25]. Material dispersion refers to the wavelength dependence of the refractive index of the material caused by the interaction between the optical mode and the material, it depends on the properties of the material itself. During the design process, the influence of the fiber structure on waveguide dispersion is an important factor in determining total dispersion. Fig. 9 shows the dispersion curve of the LP_{01} mode for both the designed NA-PCF and the structure without the nanorod assistance as a function of wavelength. It can be seen that the dispersion of NA-PCF is slightly smaller than that of non-assisted structure, whose value at 1550 nm is 14.06 ps/(nm$*$km). Table III summarizes the optical performance of the designed NA-PCF.

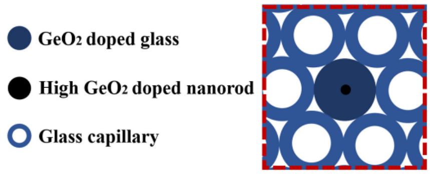

Fig. 10. The partial schematic diagram of NA-PCF preform.

V. Manufacturing of NA-PCF

For the manufacturing of hole-assisted MCFs, the most commonly used method is the stack-and-draw method [26]–[28], which can be applied to make the designed NA-PCF. For example, Xia *et al.* have successfully used the stack-and-draw method to produce hole-assisted MCF with a length of more than 1km in 2012 [10]. Fig. 10 is a schematic diagram of preparing NA-PCF by stack-and-draw method, where the high refractive index nanorods and GeO_2-doped cores can be made by vapor deposition. The core is surrounded by capillary glass tubes, and by controlling the inner diameter and the wall thickness of the capillary glass tubes, Λ_1 and d of the NA-PCF can be controlled accordingly. Another way to make NA-PCF is rod-in-tube method [29], where the core is produced by vapor deposition but the air-holes are made by drilling. The diameter of the air-hole is controlled by the diameter of the drilled hole.

VI. Conclusion

We propose a novel NA-PCF for large-capacity and long-distance transmission. Taking full advantage of the flexibility of PCF design, air-holes are arranged periodically around seven cores of a regular hexagon distribution. High refractive index nanorods are introduced to further suppress XT and increase the SMOR area without increasing λ_{cc}. A set of parameters that meet the requirements are provided as a reference. By comprehensively balancing the influence of various parameters, a set of parameters that meet the requirements are provided as a reference. The resultant NA-PCF has a XT of -50.58 dB/km and A_{eff} of 70.26 μm^2. In addition, the main optical features are investigated, where RCMF is 4.7, λ_{cc} is 1530 nm and chromatic dispersion is 14.06 ps/(nm$*$km). Stack-and-draw technique and rod-in-tube are acceptable as the fabrication methods of our design. The designed NA-PCF is expected to be applied to long-distance large-capacity transmission.

References

[1] J. Cho, X. Chen, and S. Chandrasekhar, "Trans-Atlantic field trial using high spectral efficiency probabilistically shaped 64-QAM and single-carrier real-time 250-Gb/s 16-QAM," *J. Lightw. Technol.*, vol. 36, no. 1, pp. 103–113, Jan. 2018.

[2] D. J. Richardson, J. M. Fini, and L. E. Nelson, "Space-division multiplexing in optical fibres," *Nature Photo*, vol. 7, no. 5, pp. 354–362, 2013.

[3] A. Mecozzi and R.-J. Essiambre, "Nonlinear shannon limit in pseudolinear coherent systems," *J. Lightw. Technol.*, vol. 20, no. 12, pp. 2011–2024, Jun. 2012.

[4] A. D. Ellis, J. Zhao, and D. Cotter, "Approaching the non-linear shannon limit," *J. Lightw. Technol.*, vol. 28, no. 4, pp. 423–433, Feb. 2010.

[5] J. Sakaguchi *et al.*, "305 Tb/s space division multiplexed transmission using homogeneous 19-core fiber," *J. Lightw., Technol.*, vol. 31, no. 4, pp. 554–562, Feb. 2013.

[6] A. Sano *et al.*, "409-Tb/s+409-Tb/s crosstalk suppressed bidirectional MCF transmission over 450 km using propagation-direction interleaving," *Opt. Exp.*, vol. 21, no. 14, pp. 16777–16783, 2013.

[7] B. J. Puttnam *et al.*, "2.15 Pb/s transmission using a 22 core homogeneous single-mode multi-core fiber and wideband optical comb," in *Proc. IEEE Eur. Conf. Opt. Commun.*, 2015, pp. PDP 3.1.

[8] X. Q. Xie, J. J. Tu, and X. Zhou, "Design and optimization of 32-core rod/trench assisted square-lattice structured single-mode multi-core fiber," *Opt. Exp.*, vol. 25, no. 5, pp. 5119–5132, 2017.

[9] T. Sakamoto, K. Saitoh, and N., Hanzawa, "Crosstalk suppressed hole-assisted 6-core fiber with cladding diameter of 125 μm," in *Proc. IEEE, Eur. Conf. Opt. Commun.*, 2013, pp. Mo.3.A.3.

[10] C. Xia, R. Amezcua-Correa, and N. Bai, "Hole-Assisted few-mode multi-core fiber for high-density space-division multiplexing," *Photon. Technol. Lett.*, vol. 24, no. 21, pp. 1914–1917, 2012.

[11] K. Takenaga, Y. Arakawa, and S. Tanigawa, "Reduction of crosstalk by trench-assisted multi-core fiber," in *Proc. Optical Fiber Commun. Conf. Expo. Nat. Fiber Optic Engi. Conf.*, 2011, pp. OWJ4.

[12] P., Russell, "Photonic crystal fibers," *Science,* vol. 299, no. 5605, pp. 358–362, 2003.

[13] J. W. Fleming, "Material and mode dispersion in $GeO_2{\cdot}B_2O_3{\cdot}SiC_2$ Glasses," *J. Amer. Ceram. Soc.,* vol. 59, no. 11-12, pp. 503–507, 1976.

[14] K. Takenaga *et al.*, "A large effective area multi-core fiber with an optimized cladding thickness," *Opt. Exp.*, vol. 19, no. 26, pp. B543–B550, 2011.

[15] J. R. Taylor, *Theory of Dielectric Optical Waveguides*. Cambridge, MA, USA: Academic, 1974.

[16] D. Marcuse, "Derivation of coupled power equations," *Bell Syst. Tech. J.*, vol. 51, no. 1, pp. 229–237, Jan. 1972.

[17] K. Takenaga, Y. Arakawa, and S. Tanigawa, "An investigation on crosstalk in multi-core fibers by introducing random fluctuation along longitudinal direction," *Ice Trans. Commun.*, vol. 94, no. 2, pp. 409–416, 2011.

[18] T. A. Birks, J. C. Knight, and P. S. J. Russell, "Endlessly single-mode photonic crystal fiber," *Opt. Lett.*, vol. 22, no. 13, pp. 267–274, 1997.

[19] K. Saitoh and M. Koshiba, "Empirical relations for simple design of photonic crystal fibers," *Opt. Exp.*, vol. 13, no. 1, 2005.

[20] X. Zheng *et al.*, "Bending losses of trench-assisted few-mode optical fibers," *Appl. Opt.*, vol. 55, no. 10, pp. 2639–2648, 2016.

[21] J. Tu, K. Saitoh, M. Koshiba, K. Takenaga, and S. Matsuo, "Design and analysis of large-effective-area heterogeneous trench-assisted multi-core fiber," *Opt. Exp.*, vol. 20, no. 14, pp. 15157–15170, 2012.

[22] J. Tu, K. Long, and K. Saitoh, "An efficient core selection method for heterogeneous trench-assisted multi-core fiber," *Photon. Technol. Lett.*, vol. 28, no. 7, pp. 810–813, 2016.

[23] T. Watanabe and Y. Kokubun, "Ultra-large number of transmission channels in space division multiplexing using few-mode multi-core fiber with optimized air-hole-assisted double-cladding structure," *Opt. Exp.*, vol. 22, no. 7, 2014, Art. no. 8309.

[24] S. Matsuo, Y. Sasaki, and T. Akamatsu, "12-core fiber with one ring structure for extremely large capacity transmission," *Opt. Exp.*, vol. 20, no. 27, Art. no. 28398, 2012.

[25] S. Haxha and H. Ademgil, "Novel design of photonic crystal fibres with low confinement losses, nearly zero ultra-flatted chromatic dispersion, negative chromatic dispersion and improved effective mode area," *Opt. Commun.*, vol. 281, no. 2, pp. 278–286, 2008.

[26] R. G. H. Van Uden, R. A. Correa, and E. A. Lopez, "Ultra-high-density spatial division multiplexing with a few-mode multicore fibre," *Nature Photon*, vol. 8, no. 11, pp. 865–870, 2014.

[27] A. Ziolowicz *et al.*, "Hole-assisted multicore optical fiber for next generation telecom transmission systems," *Appl. Phys. Lett.*, vol. 105, no. 8, 2014, Art. no. 081106.

[28] I. Ishida, "Possibility of stack and draw process as fabrication technology for multi-core fiber," in *Proc. IEEE. Opt. Fiber Commun. Conf. Expo. Nat. Fiber Optic Engineers Conf.*, 2013, pp. OTu2G.1.

[29] T. Hayashi, T. Taru, O. Shimakawa, T. Sasaki, and E. Sasaoka, "Design and fabrication of ultra-low crosstalk and low-loss multi-core fiber," *Opt. Exp.*, vol. 19, no. 17, pp. 16576–16592, 2011.